CrossMark

A broadband core shift polarization filter based on photonic crystal fiber with a big gold-coated air hole

Xinxing Feng[1] · Huijing Du[1] · Shuguang Li[1] · Yinan Zhang[1] ·
Qiang Liu[1] · Xinyu Gao[1]

Abstract We propose a modified design for a Core shift photonic crystal fiber (PCF) polarization filter based on surface plasmon resonance. The Core shiftting is achieved by the air holes with different diameters around the gold-coated holes, which can separate the refractive index of the x-polarization and y-polarization second order surface plasmon polariton modes. The influences of structural parameters of the PCF on the filter characteristics are studied using the finite element method. Simulation results great changes have taken place in the results of numerical simulation by changing the thickness of the gold film and air hole diameter. We obtain a resonance wavelength with 1550 nm. The y-polarization mode is supressed significantly with the loss of 58,456.7 dB/m. With the length of the fiber is 300 μm, a extinction ratio is higher than 20 dB and a bandwidth achieve to 450 nm at the communication wavelength can be got. All these properties we achieved in the core shift PCF are important properties of PCF in broadband polarization filter in application. Our design can offer some guidance to the production of the polarization filter.

Keywords Photonic crystal fiber · Surface plasmon resonance · Polarization
filter

1 Introduction

Surface plasmon resonance (SPR) is a kind of physical phenomena, when the incident light with critical angle is coupled to the medium interface of two different refractive indexes, the light can cause the resonance of metal free electrons. Because the free electrons can absorb light energy, reflect light in certain angle will greatly abate.

✉ Shuguang Li
shuguangli@ysu.edu.cn

[1] Key Laboratory of Metastable Materials Science and Technology, College of Science, Yanshan University, Qinhuangdao 066004, People's Republic of China

Photonic crystal fibers (PCFs; Russell 2003; Kuhlmey et al. 2006; Koshiba 2002; Koshiba and Tsuji 2000; Hansen et al. 2001; Birks et al. 1997), which are also called holey fibers or microstructure optical fibers, have attracted considerable interest due to their unique advantages, such as high-birefringence, low loss, big mode area and so on. PCFs are divided into two kinds of fibers. The first one is index-guided PCF, guiding light by total internal reflection between a high refractive index core and a low refractive index cladding region. The other one is photonic-bandgap PCF, guiding light by the photonic bandgap in a low refractive index core-region. In this paper, index-guided PCF is employed. Many functional devices based on PCF, including polarization splitters (Liu et al. 2015), sensors (Liu et al. 2015), rotators (Hameed and Obayya 2011), wavelength division multiplexer (WDM; Chen et al. 2009), laser (Rosenstein et al. 2014) and amplifiers (Robin et al. 2014), have been proposed. The characteristics of PCF could be changed by filling the cladding air holes with liquid, liquid crystal (Kuo et al. 2011), semiconductor, mental (Morishita and Miyake 2004; Schmidt and Russell 2008; Gauvreau et al. 2007), oil, and so on. In recent years, the method of metal-layer coating on the inner wall of the air hole has been developed quite rapidly. When the phase matching condition of the optical model and the metal surface free electrons is satisfied, the coupling is happened, a kind of near field electromagnetic wave is produced and propagates along the metal surface which leads to that electromagnetic field energy is efficiently into the collective of free electrons on the metal surface and has a lot of losses. In this article, the coupling between y-polarization and SPP mode is strongest in 1550 nm, which results that the refractive index increases suddenly and loss reaches the peak at the same time. The resonance wavelength can be modulated by the thickness, position, and permittivity of the metal layer in the fiber.

Nowadays, PCF manufactured technology is developing very rapidly, producing method and diversity, including ultrasonic drilling, casting rod tube, extrusion and stack. One metal spraying methods including metal nanoparticle hybrid fiber inhalation and evaporation. Therefore, the PCF filter coated metal film with simple structure can be fabricated in reality (Morishita and Miyake 2004).

In this paper, we propose a PCF polarization filter with gold-coated by the finite element method. The PCF air holes are arranged in a hexagonal lattices, and the air holes are arranged in a diamond. The core modes couple to the SPP modes when the phase-matching conditions are satisfied. By making the PCF with high birefringence, the resonance wavelengths of x-polarization mode and y-polarization mode can be divided. In order to adjust the resonant wavelength in the y-polarization to 1550 nm, we adjust the thickness of gold layer to 26.5 nm, the loss of y-polarization mode is further larger than that of x-polarization mode at 1550 nm. When the fiber length is 300 μm, the value of extinction ratio reaches to 152.3 dB. The PCF we proposed has a simple structure and a big relatively large margin of error. The fiber is easy to control and applicable for fiber filter production.

2 The structure and basic theory

The cross section of the proposed PCF is shown in Fig. 1. The background material of the fiber is pure silica, whose dispersion relationship is calculated by the Sellmeier equation (Schmidt and Russell 2008). The background material of this fiber is silicon, and the little and big cross section diameter is 30 and 40 μm. The air holes are arranged in a hexagonal lattice, the diameter of the white air holes d equals to 2.4 μm, and the effective refractive index of air is set as 1. The lattice pitch is represented by $\Lambda = 3.0$ μm. The diameters of

Fig. 1 Cross-section of the designed photonic fiber filters
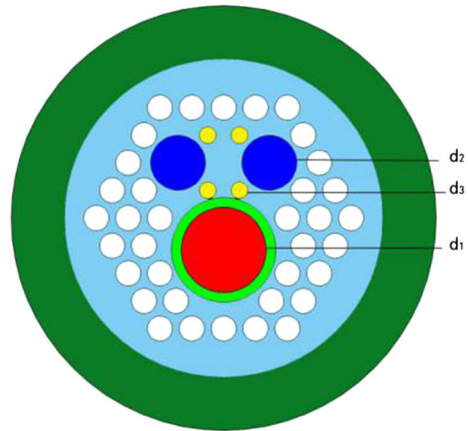
the red air holes and the thickness of the gold layer are represented by $d_1 = 9.8$ μm and $t = 26.5$ nm, the blue air hole are represented by $d_2 = 5.2$ μm, the yellow air hole are represented by $d_3 = 1.6$ μm.

The chromatic dispersion of the background material, which is pure silica, and is calculated by the sellmeier equation (Lee et al. 2008). Likewise, the dielectric constant of the gold is also characterized by the Drude–Lorentz model (Vial et al. 2005) and could be expressed as:

$$\varepsilon_m = \varepsilon_\infty - \frac{\omega_D^2}{\omega(\omega + j\gamma_D)} - \frac{\Delta\varepsilon \cdot \Omega_L^2}{(\omega^2 - \Omega_L^2) + j\Gamma_L\omega} \tag{1}$$

where $\varepsilon_m = 5.9673$ is the permittivity of the gold, $\Delta\varepsilon = 1.09$ can be interpreted as a weighting factor, and is the angular frequency of guided light, ω_D and γ_D are the plasma frequency and damping frequency, $\omega_D/2\pi = 2113.6$ THZ; $\gamma_D/2\pi = 15.92$ THZ. Ω_L and Γ_L represent the frequency and the spectral width of the Lorentz oscillator. $\Omega_L/2\pi = 650.07$ THZ; $\Gamma_L/2\pi = 104.86$ THZ.

The mode loss can be defined as:

$$L = 8.686 \times \frac{2\pi}{\lambda}\text{Im}(n_{eff}) \times 10^4 \tag{2}$$

where units of the loss and wavelength are dB/m and μm respectively; the Im[neff] is the imaginary part of the effective refractive index (Vial et al. 2005).

In this paper, the perfect matching layer (PML; Gauvreau et al. 2007) and a scattering boundary are used. While the phases of the SPPs mode and the core mode match. The energy in the core of the PCF can strongly couple to the surface plasmon of the metallic nanotubes. And the loss peaks are formed where the coupling occurs.

3 Numerical result and analysis

The cross section of the proposed polarized filtering PCF with nanoscale gold film is shown in Fig. 1. We achieve the optimization results at the communication wavelength of 1550 nm. Figure 2 shows the dependence of effective index on wavelength of
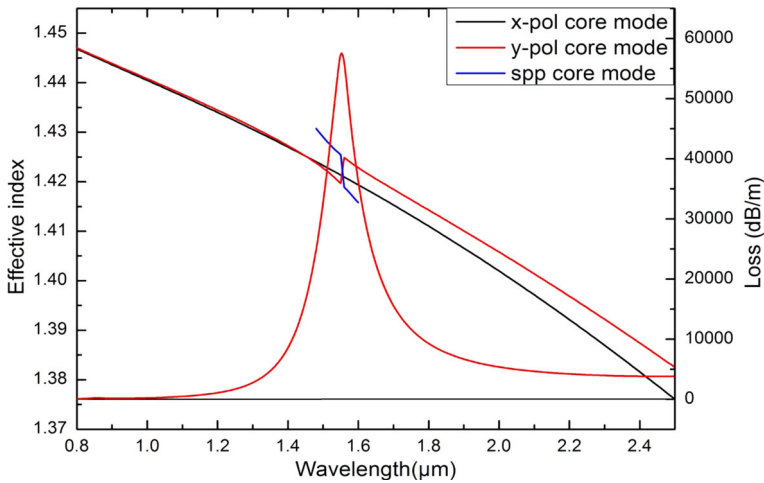
Fig. 2 Wavelength dependence of effective indices and losses of x-polarization and y-polarization core modes in the PCFs

x-polarization and y-polarization core modes. In this part, d = 2.4 μm, d_1 = 9.8 μm, d_2 = 5.2 μm, d_3 = 1.6 μm, the thickness of the metal film is t = 26.5 nm.

The black thread and the red line on the x-polarization and y-polarization mode respectively from the fiber core mode effective index and loss. The blue dotted line represents the second order SPP mode in y-polarization. We see that The refractive index decreases gradually with the increase of wavelength, and y-polarization of the refractive index of y-polarization had a sudden increase in the 1550 nm, and the loss reached the maximum value of the y-polarization mode are 58,456.7 dB/m, at the same time, the x-polarization mode is only 9.9 dB/m. As we can see, the difference between the effective index of x-polarization and that of y-polarization is quite small. These two lines almost coincide with each other. So the birefringence is not high at all. Moreover, it is evidently that the reason of the difference between the x-polarization resonance wavelength and the y-polarization resonance wavelength is the apart of the second SPP mode instead of the birefringence. When the optical modes meets metal nanoparticles and the incident photonic frequency matches with the metal nanoparticles, nanoparticles can produce very strong absorption of photon energy, the local surface plasmon resonance occurs and fiber mode produces loss peak at this time.

To our knowledge, the resonance properties can be easily affected by the structural parameters such as the thickness of the metal film, diameters of the air holes in the cladding layer, and so on. We realize a polarized filtering PCF by modulation the structural parameters of the PCF coated by nanoscale gold film, which can filter out y-polarization core mode. To constrain the light in the fiber core and ensure the efficient transmission properties of fiber, the structure parameters must be set at the same order of magnitude as the wavelength. The effective refractive index of core mode or SPP mode is varying with the variations of parameters. And we can adjust the parameters in order to meet the different need. In this paper, we adjust the SPP mode by changing the thickness of the gold film and the diameter of d_1, d_2 and d_3. Now, we will discuss the impact of the parameters mentioned above on the loss.
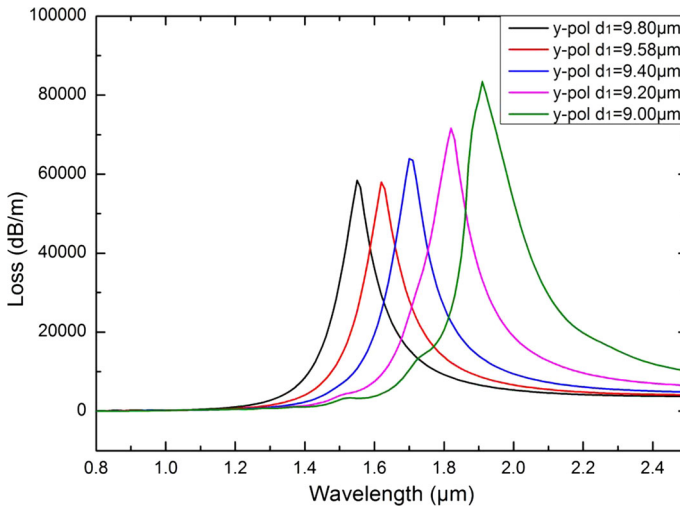
Fig. 3 Changes of the confinement loss peaks in the y-polarization core mode with different diameters of d_1

Figure 3 is by changing the diameter of air hole d_1. At this time, the diameter of the air holes are respectively 9.00, 9.20, 9.40, 9.58 and 9.80 μm. Figure data changes in the trend is clear. With the air hole diameter reduction, the loss of y-polarization decreases from 83,417.9 to 58,456.7 dB/m. At the same time loss of peak value moved towards the short wavelength, the resonance wavelength moved from 1910 to 1550 nm. So we can change the diameter of the d_1 to adjust the peak value of the loss of y-polarization.

Figure 4 is based on Fig. 1 by changing the diameter of air hole d_2, At this time, $d_1 = 9.80$ μm, $d_3 = 1.6$ μm, the diameter of the air holes are respectively 4.00, 4.40, 4.80 and 5.20 nm. We can see from the picture, the y-polarization core mode loss is not only determined by the size of d_1, more related to the diameter of the d_2. The bigger the
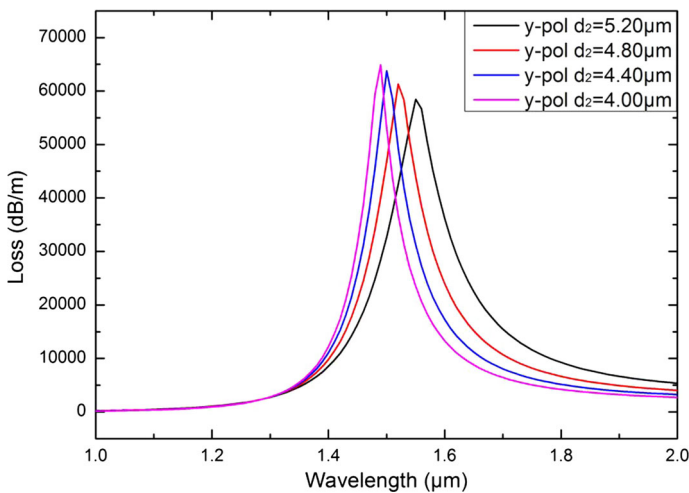

Fig. 4 Changes of the confinement loss peaks in the y-polarization core mode with different diameters of d_2

diameter of the d_2, the smaller the loss of the y-polarization core mode. Peaks of the loss of y-polarization at the same time has a tendency to move short wavelength. With the increase of the size of the d_2, the contact area increased both the core mode and the metal film. So will increase the losses in the y-polarization.

Besides the diameter of d_1, d_2, the size of the d_3 and polarization filter performance is also relevant. So in Fig. 5 the diameter of the air holes are respectively 1.20, 1.30, 1.40, 1.50 and 1.60 μm. With the decrease of air hole size, A huge decrease in losses in the y-polarization, the loss peak from 1550 to 2010 nm, and the loss is gradually decreasing from 58,456.7 to 34,762.7 dB/m. So, with the increase of d_3 diameter the loss gradually increases, the peak red shift at the same time.

Several studies show that surface plasmon waves are very sensitive to the thickness of the metal layer. So the Fig. 6 is on the basis of Fig. 1 by changing the thickness of the metal film, which respectively is 16, 20, 26.5, 30, 40 and 50 nm. With the increase of the thickness of the metal film, y-polarization of the loss peak gradually moves toward the long wavelength, the resonance wavelength moved from 1550 to 1900 nm, and there is a huge loss peak growth. The loss of peak when gold film thickness is 50 nm to 90,619.2 dB/m, It has huge benefits to the promotion of filter performance.

Figure 7 Show the loss of mode dependence on the operable wavelength λ when a complete coupling happens. As the wavelength increases, the core mode and SPP mode couple to each other and split into another new modes. For lower curve, mode field is mainly distributed in the core region at the short wavelength, mode field begins to transfer from core region to gold-film region as wavelength increases, the field intensity in the core region is same as the field intensity in the gold-film region at the turn of the curve, and almost all the field transfers from core region to gold-film region at the longer wavelength. The mode transition of the upper curve is contrary to that of the lower curve. The mode transition from core mode to SPP mode also happens to the losses. For the black curve, mode loss follows core mode at the short wavelength, and follows SPP mode at the long wavelength. There is a intersection between the black curve and red curve. At the
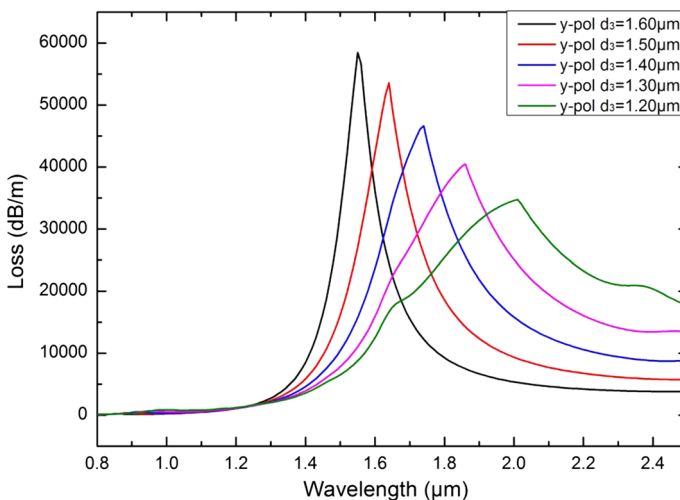

Fig. 5 Changes of the confinement loss peaks in the y-polarization core mode with different diameters of d_3
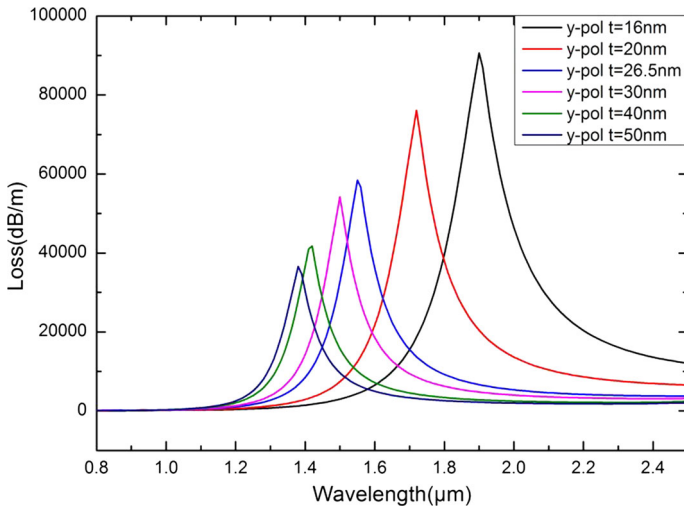
Fig. 6 Filter characteristics of PCFs with different gold-coated layers. The *solid lines* of different colors are the loss of core modes in the y-polarization. (Color figure online)
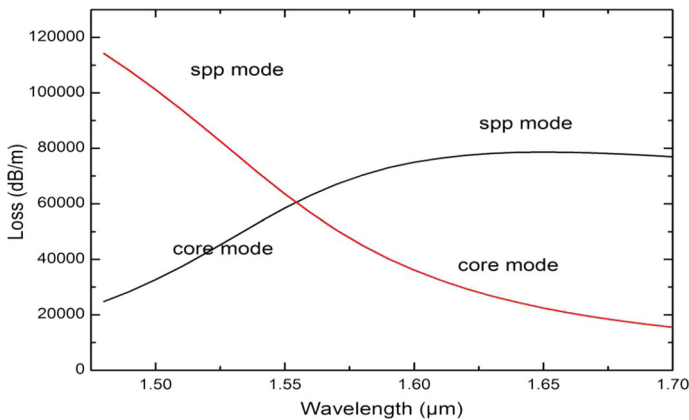

Fig. 7 The loss of the mode dependence on the operable wavelength λ when a complete coupling happens

intersection, the losses of the two modes are equal. The intersection corresponds to the turn of the curve in Fig. 7. This coupling is called complete coupling (Fig. 8).

Big loss is helpful for polarization filter to filter out one polarized mode. The structure could be further improved for better effect. The polarization filter could be used for the communication windows of 1550 nm which can be used for carrying data/voice and video respectively. In addition, extinction ratio (ER) is a key element for polarization filter. And it can be calculated by following equation:

$$ER = 20 \lg\{\exp[(\alpha_2 - \alpha_1)L]\} \tag{3}$$

where α_1 and α_2 represent the loss of x-polarized and y-polarized, respectively. L is the length of fiber (Lee et al. 2008). Now we set the value of L as 100, 200 and 300 μm. From the picture we can find that when the length of the fiber is 300 μm, the extinction ratio is
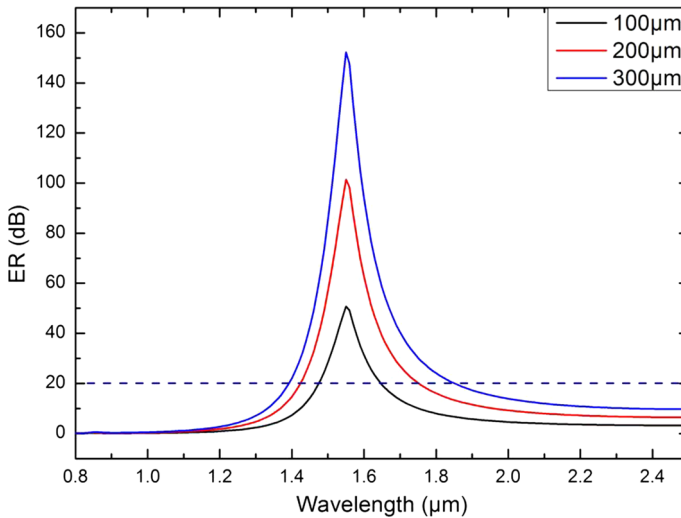
Fig. 8 The extinction ratio curve with Fig. 2

better than 20 dB to achieve to 152.3 dB and the bandwidth is about 450 nm. This is very advantageous to make broadband filter. More importantly, the length of the photonic crystal fiber is very short, which can be used to micro integration.

4 Conclusion

In this paper, we investigated the coupling characteristics and the polarization character-istics of the proposed PCF with nanoscale gold film through the full vector finite element method (FV-FEM) with perfectly matched layers (PMLs). The coupling theory between core mode and SPP mode is introduced. The resonance strength and the impacts of structural parameters of the photonic crystal fiber on the polarization filter characteristics are studied. Simulation results show that the resonance wavelength is in communication wavelength 1550 nm, the loss of the y-polarization is 58,456.7 dB/m, when the length of the fiber is the 300 μm, extinction ratio is more than 20 dB and the wavelength range is from 1400 to 1850 nm. We think this PCF polarization filter could be used widely in the develop of integrated, large-capacity, broad-bandwidth optical communication system.

References

Birks, T., Knight, J., Russell, P.: Endlesslysingle-modephotonic crystal fiber. OSA Opt. Lett. **22**(13), 961–963 (1997)
Chen, M.Y., Zhou, J., Pun, E.Y.: A novel WDM component based on a three-core photonic crystal fiber. J. Lightwave Technol. **27**(13), 2343–2347 (2009)
Gauvreau, B., Hassani, A., Fassi Fehri, M., Kabashin, A., Skorobogatiy, M.A.: Photonic bandgap fiber-based surface plasmon resonance sensors. Opt. Express **15**(18), 11413–11426 (2007)

Hameed, M.F.O., Obayya, S.S.A.: Design of passive polarization rotator based on silica photonic crystal fiber. Opt. Lett. **36**(16), 3133–3135 (2011)

Hansen, T.P., Broeng, J., Libori, S.E.B., Knudsen, E.: Highly bire-fringent index-guiding photonic crystal fibers. IEEE Photon. Technol. Lett. **13**(6), 588–590 (2001)

Koshiba, M.: Full-vector analysis of photonic crystal fibers using the finite element method. IEICE Trans. Electron. **85**(4), 881–888 (2002)

Kuhlmey, B.T., Pathmanandavel, K., McPhedran, R.C.: Multipole analysis of photonic crystal fibers with coate dinclusions. Opt. Express **14**(22), 10851–10864 (2006)

Kuo, S.M., Huang, Y.W., Yeh, S.M., Cheng, W.H., Lin, C.H.: Liquid crystal modified photonic crystal fiber (LC-PCF) fabricated with an un-cured SU-8 photoresist sealing technique for electrical flux measurement. Opt. Express **19**(19), 18372–18379 (2011)

Lee, H., Schmidt, M., Tyagi, H., Sempere, L.P., Russell, P.S.J.: Polarization-dependent coupling to plasmon modes on submicron gold wire in photonic crystal fiber. Appl. Phys. B **93**(11), 12180–12189 (2008)

Liu, Q., Li, Q., Fan, Z., Zhang, W., Li, H., Zi, J., An, G.W.: Numerical analysis of ultrabroadband polarization splitter based on gold-filled dual-core photonic crystal fiber. Opt. Commun. **334**, 46–50 (2015a)

Liu, Q., Li, S.G., Chen, H.L., Fan, Z., Li, J.S.: Photonic crystal fiber temperature sensor based on coupling between liquid-core mode and defect mode. IEEE Photon. J. **7**(2), 1–9 (2015b)

Morishita, K., Miyake, Y.: Fabrication and resonance wavelengths of long-period gratings written in a pure-silica photonic crystal fiber by the glass structure change. J. Lightwave Technol. **22**(2), 626–630 (2004)

Robin, C., Dajani, I., Pulford, B.: Modal instability suppressing, single-frequency photonic crystal fiber amplifier with 811 W output power. Opt. Lett. **39**(3), 666–669 (2014)

Rosenstein, B., Shirakov, A., Belker, D., Ishaaya, A.A.: The 0.7 MW output power from a two-arm coherently combined Qswitched photonic crystal fiber laser. Opt. Express **22**(6), 6416–6421 (2014)

Russell, P.: Photonic crystal fibers. Science **299**(5605), 358–362 (2003)

Schmidt, M.A., Russell, PStJ: Long-range spiralling surface plasmon modes on metallic nanowires. Opt. Express **16**(18), 13617–13623 (2008)

Tsuji, Y., Koshiba, M.: Curvilinear hybrid edge/nodal elements with triangular shape for guided-wave problems. J. Lightwave Technol. **18**(5), 737–743 (2000)

Vial, A., Grimault, A.-S., Macias, D., Barchiesi, D., de Chapelle, M.L.: Improved analytical fit of gold dispersion: application to the modeling of extinction spectra with a finite-difference time-domain method. Phys. Rev. B **71**(8), 085416–085423 (2005)